

## Irradiated Stainless Steel Crack-Growth-Resistance Curves

J. Bernard, G. Verzeletti

*Commission of the European Communities, J.R.C. Ispra Establishment, Applied Mechanics Division,  
I-21020 Ispra, Italy*

### Abstract

A study of the neutron damage suffered by the AISI 316H steel commonly used in the construction of LMFBR primary circuit irremovable components is conducted at the JRC of Ispra. The fast fluences ( $E > 0.1$  MeV) foreseen to be investigated cause neutron damage from 0.1 dpa to 2 dpa. Tests are run at 350°C and 550°C on base, welded and heat-affected-zone material. To characterize the EPFM behaviour of the metal, J-R crack-growth-resistance curves are elaborated. Results are given corresponding to the nought, 0.1 dpa, 0.3 dpa and 1 dpa irradiations. Tests are run in air at a temperature corresponding to the one the specimens sustained during irradiation in sodium filled capsules. Only four three point bend specimens are available per case studied. Determining J-R curves was done using a key-curve based method together with J-like parameters, an approach that yielded satisfactory results when applied to subsized specimens.

### 1. Introduction

When tackling a FM study on irradiated materials, some problems arise deriving from limitations set by the irradiation facility. They concern the specimen size and the low number of tests that can be carried out per case studied; a case being characterized by the material (base, weld or heat affected zone metal), the fluence and the test temperature (350°C or 550°C). In order to elaborate crack-growth-resistance curves, an experimental and analytical approach was opted for that uses a dimensional analysis based determination of current crack length together with J-like parameters. In the course of this research, these concepts have been in part revised so as to be directly applicable to the three point bend (3PB) specimens configuration used throughout this work. The procedure yields consistent J-R curves for the base and the weld material. Concerning the HAZ metal, all results have, as lower bounds, the weld metal J-R curves at 550°C and at a given neutron damage, and these results will not be further discussed here.

### 2. Materials and Specimen Preparation

The 3PB specimens are cut from a 50 mm thick AISI 316H stainless steel plate. The material is in the fully annealed condition (1/2 h at 1080°C and quenched in water). The welded specimens are machined from a non-annealed welded assemblage consisting in two strips cut from the plate and butt-welded together following the MIG procedure. The chemistry of the

base metal and of the weld deposit is given in Table 1. The mechanical properties of the non-irradiated steel appear in Table 2. The 3PB specimen dimensions used appear in Fig. 1. The longitudinal axis of the specimen is parallel to the plate rolling direction (standard L-S type of specimen). Two types of specimens are distinguished according to the material into which the crack propagates, that is, base material (B specimens) and weld material (W specimens). Fatigue precracking of the specimens to a nominal initial crack length to width ratio of 0.55 was accomplished in amplitude control of the load point displacement (20 Hz sinusoidal wave). Details on the precracking and a description of the irradiation facility appear in [1].

### 3. Experimental Apparatus and Procedures

The hot cell set-up includes a 50 KN Instron machine and the out-of-cell one a servo-hydraulic 63 KN Schenck machine. The testing rig is identical in both installations. A Hewlett-Packard 1000 data acquisition system (DAS) records in digital form the applied force, two displacements, the average of which corresponds to the load point displacement of the cracked body and two potentiometric signals indicating incipient crack growth using the direct current potential drop (DCPD) technique. The DAS picks up signals at equispaced time intervals of 200 ms at the most. Measurements of initial and final crack length is based on the nine-point average method using photographs of the fracture surface, after heat-tinting at 550°C for several minutes. The magnification factor is four and the resolution is about  $\pm 25 \mu\text{m}$

### 4. Current Crack Length Calculation

Applying the dimensional analysis arguments proposed by Rice [2] to deeply cracked specimens in bending leads to the following relationship between the plastic angle  $\theta_{pl}$ , the applied moment  $M$  and the current ligament size  $b$ , provided that plasticity is confined to the ligament area:

$$M = b^2 F(\theta_{pl}) \quad (1)$$

Equation (1) calls for the following comments:

- 1) Under the form  $M/b^2 = F(\theta_{pl})$  it is akin to a monotonic stress-strain relationship depending only on material properties. In this research,  $F(\theta_{pl})$  will thus vary according to what material is considered (B or W), the test temperature and the degree of neutron damage suffered.  $F(\theta_{pl})$  is referred to as a material "key curve".
- 2) The relationship (1) is sufficiently accurate when the current crack length ( $a$ ) to width ( $W$ ) ratio is  $a/W \geq 0.5$  and for the standard 3PB specimen having a span  $s$  to  $W$  ratio of four [3]. In our study the initial  $a_0/W$  after precracking was set at 0.55.
- 3) Equation (1) is an implicit relationship between current ligament length  $b$  and the parameter  $M$  (or equivalently, applied load) and  $\theta_{pl}$  (or equivalently, plastic part of the load point displacement).

The third comment provides the clue to the determination of the current crack length  $a = W - b$ . Indeed, the  $F(\theta_{pl})$  can be determined, in theory, using specimens having smaller ligaments than the one of our reference specimen, but specific problems inherent to the

study of a relatively limited number of irradiated specimens necessitated a different approach to define  $F(\theta_{pl})$ . The problem was addressed as follows. If  $b_0$  is the initial ligament length and  $b$  is the current ligament length, then at the end of a test,  $b = b_f$ , is known from heat-tinting measurements (see section 3). It may be observed that in a first approximation, the key curve is composed of (see Fig. 2):

- 1) An initial part which is identical to the measured experimental data  $M/b_0^2$  versus  $\theta_{pl}$ ; since for the low  $\theta_{pl}$  values no crack growth takes place and  $b = b_0$ , the initial ligament length, and (1) simply equates to

$$\frac{M}{b_0^2} = F(\theta_{pl}) \quad (2)$$

- 2) A tangent to this initial curve passing through a point  $M/b_f^2, \theta_{pl}$  where  $M, b_f$  and  $\theta_{pl}$  are measured end of test values. Indeed, and by equation (1),  $M/b_f^2$  is the value of the key curve function  $F(\theta_{pl})$  at the corresponding  $\theta_{pl}$ .

Since the key curve is akin to a stress-strain curve, it must be a smooth curve, therefore the tangent is the best approximation for a more or less downward concave curve merging into the initial  $M/b_0^2 = F(\theta_{pl})$  part.

It has been observed, for all tests run on B and W material, that the four (per case studied) simplified key curves constructed as described, can be superposed in a most satisfactory manner. For example, the points of tangency correspond to a fairly constant  $\theta_{pl}$  and the four end of test points align reasonably well on a unique tangent. It is implicit that the initial  $M/b_0^2$  versus  $\theta_{pl}$  curves do correspond. This is illustrated in Fig. 3. Having defined an appropriate key curve function, the current crack length can now be calculated using straightforward data reduction procedure. The steps are:

- 1) Calculation of the  $F(\theta_{pl})$  function, which requires the calculation of a line passing through an experimentally determined point and that is tangent to an experimentally defined normalized moment ( $M/b_0^2$ ) versus plastic part of the angular displacement  $\theta_{pl}$  curve.
- 2) Calling the normalized  $M/b_0^2$  versus  $\theta_{pl}$  curve the  $F'$  curve and identifying the key curve as the  $F$  curve, then equation (1) yields:

$$F_i = \frac{M_i}{b_i^2} \quad (3)$$

and

$$F'_i = \frac{M_i}{b_0^2} \quad (4)$$

where the subscript  $i$  refers to the specific point at which  $b_i$  is being evaluated. From (3) and (4) it follows that

$$b_i = b_0 (F'_i/F_i)^{0.5} \quad (5)$$

therefore an incremental increase of the current crack length  $a$  between stage  $i$  and  $i+1$

follows from (5). Indeed

$$a_{i+1} - a_i = b_0 \left[ (F'_1/F_1)^{0.5} - (F'_{i+1}/F_i)^{0.5} \right] \quad (6)$$

### 5. Elaboration of J-Resistance Curves

The candidate J-like field parameter used in a first analysis of the test results is the deformation theory  $J = J_D$ . In the case of specimens submitted to bending loads it is defined as [4]

$$J_D = 2 \int_0^{\theta_c} \frac{M}{b} d\theta_c - \int_{a_0}^a \frac{J_D}{b} da \quad (7)$$

where

- M = applied moment per unit thickness
- a = current crack length
- b = current ligament length
- b = W-a where W = 20 mm is the specimen width
- a<sub>0</sub> = initial crack length = W-b<sub>0</sub>
- θ<sub>c</sub> = rotation of the cracked specimen

Equation (7) is widely used when the crack growth is J-controlled. The criteria to be met are:

Firstly,  $\frac{\Delta a_{\max}}{b} < 10\%$  where Δa is the maximum crack extension;

Secondly, a parameter  $\omega = \frac{b}{J} \cdot \frac{dJ}{da} \gg 1$ .

For  $\omega = 5$  [5] and  $\Delta a < 900 \mu\text{m}$  it has been shown [6] that the tests have indeed been run to the maximum J-controlled growth capacity of the specimens.  $J_D$ -R curves that have been elaborated appear in Figs. 4 and 5. Recently, a modified J has been introduced,  $J_M$  [7], allowing to exploit results of tests for which  $0.1 < \Delta a_{\max}/b < 0.3$ . The J-R curves obtained are quite consistent with those elaborated using much larger-sized specimens. The definition of  $J_M$  is

$$J_M = J_D - \int_{a_0}^a \frac{\partial J}{\partial a} \bigg|_{\theta, p\ell} da \quad (8)$$

where  $J_{p\ell}$  is the plastic part of the deformation theory  $J_D$ . Differentiating expression (7) and separating  $J_D$  in its elastic and plastic parts yields

$$dJ_D = \frac{2M}{b} d\theta_{el} - \frac{G}{b} da + 2 \frac{M}{b} d\theta_{p\ell} - \frac{J_{p\ell}}{b} da \quad (9)$$

where G is the Griffith linear elastic energy release rate. Hence

$$d J_{p\ell} = \frac{2M}{b} d\theta_{p\ell} - \frac{J_{p\ell}}{b} da \quad (10)$$

Dividing both sides of equation (10) by  $b$  and integrating leads to

$$J_{p\ell} = 2b_i \int_0^{\theta_{p\ell}} \frac{M}{b^2} d\theta_{p\ell} \quad (11)$$

where the subscript  $i$  refers to the specific step at which the integral is evaluated.

From dimensional analysis (see section 4):

$$\frac{M}{b^2} = F(\theta_{p\ell})$$

Therefore partial differentiation of (11) with respect to  $a$  and at the current  $\theta_{p\ell}$  leads to

$$\left. \frac{\partial J_{p\ell}}{\partial a} \right|_{\theta_{p\ell}} = - \frac{J_{p\ell}}{b} \quad (12)$$

From (8)

$$dJ_M = dJ_D - \left. \frac{\partial J_{p\ell}}{\partial a} \right|_{\theta_{p\ell}} da \quad (13)$$

Hence, from (9), (12) and (13):

$$dJ_M = 2 \frac{M}{b} d\theta - \frac{G}{b} da \quad (14)$$

Integration of (14) yields

$$J_M = 2 \int_0^{\theta} \frac{M}{b} d\theta - \int_{a_0}^a \frac{G}{b} da \quad (15)$$

in the case of deeply cracked 3PB specimens. For 3PB specimens:

$$G = \frac{CP^2}{bB} [8] \quad (16)$$

where  $C$  is the specimen compliance and  $P$  is the applied load,  $b$  the current ligament and  $B$  the thickness ( $B = 15$  mm).  $C = C_0$ , before crack initiation, is derived from the initial elastic load-displacement measurements. Knowing the current crack length  $a$  (see section 4), the current  $C = C_i$  is calculated using the compliance functions  $V(a/w)$  [9]

$$C_i = C_0 \frac{V_i(a/w)}{V_0(a_0/w)} \quad (17)$$

where the subscript  $i$  refers to the specific points at which the compliance is evaluated.

One example of  $J_M$  calculation is given in Fig. 6. The branching of the  $J_D$ - $R$  curve from the  $J_M$ - $R$  curve is manifest after some crack extension and derives from the  $2^d$  term in the right-hand side of equation (7), being an overcorrection in the case of specimens in bending.

## 6. Conclusions

The dimensional analysis based calculations of the current crack lengths together with the use of the deformation theory of plasticity defined  $J$  have been found to be efficient in elaborating consistent  $J$ - $R$  curves for subsized 3PB specimen in AISI 316H and for crack growths limited to 900  $\mu\text{m}$ . Introducing the  $J_M$  integral, revised so as to be applicable to the 3PB specimens used throughout this research, is of interest since tests where greater crack extensions are attained may be exploited. Considering the fact that the research as planned has reached roughly the halfway point, future work will clearly benefit from the application of  $J_M$ .

## Acknowledgements

The authors wish to thank the following persons: Messrs. Manzotti and Tognoli, Applied Mechanics Division, JRC-Ispira, who performed the calibrations and the measurements; Dr. Lölgen and co-workers from HFR, JRC-Petten, for their work concerning the irradiation of the test specimens.

## References

- [1] BERNARD, J. and VERZELETTI, G., "Experimental determination of fracture mechanics parameters of irradiated materials", Advanced Seminar on Fracture Mechanics (ASFM4), JRC Ispira, October 24-28, 1983. To be published in 1985 by D. Reidel Publishing Co., L.H. Larsson, Editor, pp.145-164.
- [2] RICE, J.R., PARIS, P.C. and MERKLE, J.G., in "Progress in flaw growth and fracture toughness testing", ASTM STP 536, American Society for Testing and Materials, 1973, pp.231-235.
- [3] ERNST, H., PARIS, P.C., ROSSON, M. and HUTCHINSON, J.W., "Analysis of load-displacement relationships to determine  $J$ - $R$  curve and tearing instability material properties", Fracture Mechanics, ASTM STP 677, C.W. Smith, Ed., American Society for Testing and Materials, 1979, pp.581-599.
- [4] HUTCHINSON, J.W. and PARIS, P.C., "Stability analysis of  $J$  controlled crack growth", Elastic-Plastic Fracture, ASTM STP 668, J.D. Landes, J.A. Begley and G.A. Clarke, Eds., American Society for Testing and Materials, 1979, pp.37-64.
- [5] PARIS, P. and JOHNSON, R., "A method of application of elastic-plastic fracture mechanics to nuclear vessel analysis", Seminar on EPPM, sponsored by IWM, Freiburg (Germany) June 1981.
- [6] BERNARD, J. and VERZELETTI, G., "Elasto-plastic fracture mechanics characterization of type 316H irradiated stainless steel up to 1 dpa", Symp. on the Effects of Radiation on Materials, to be published in ASTM STP 870, F.A. Garner and J.S. Perrin, editors.
- [7] ERNST, H.A., "Material resistance and instability beyond  $J$ -controlled crack growth", Elasto-Plastic Fracture: Second Symp. ASTM STP 803, C.F. Shih and J.P. Gudas, editors, ASTM, 1983.
- [8] SUMPTER, J.D.G. and TURNER, C.E., "Method for laboratory determination of  $J_C$ ", Cracks and Fracture, ASTM STP 601, American Society for Testing and Materials, 1976, pp.3-18.
- [9] TADA, H., PARIS, P. and IRWIN, G., "The stress analysis of cracks Handbook", Del Research Corporation.

TABLE 1 - Chemical composition of the investigated steel in weight percent

Base material	C	Si	Mn	P	S	Cr	Ni	Mo	Co
	0.056	0.34	1.61	≤ 0.02	0.009	15.2	12.1	2.44	0.06
	Ti	Nb	Cu	B	V	N			
	≤ 0.005	≤ 0.005	0.22	0.00097	0.087	0.082			
Weld material	C	Si	Mn	P	S	Cr	Ni	Mo	Co
	0.051	0.43	2.25	≤ 0.02	0.009	16.0	8.9	2.36	0.06
	Ti	Nb	Cu	B	V	N			
	≤ 0.005	≤ 0.005	0.17	0.00088	0.08	0.082			

TABLE 2 - Mechanical properties of the non-irradiated steel

Material	Temperature °C	Yield strength MPa	Ultimate tensile strength MPa	Uniform elongation percent
Base	20	240 <sup>a</sup>	570 <sup>a</sup>	65 <sup>a</sup>
Base	350	133	483	36
Base	550	105	440	35
Weld	350	300	445	16
Weld	550	250	382	14

<sup>a</sup> Result obtained in one test on a  $\phi$  4 mm tensile specimen, gauge length was 20 mm.

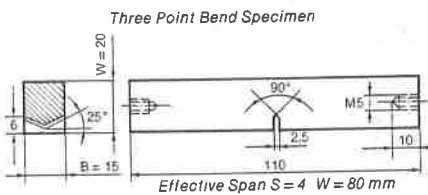


Fig. 1 - Dimension of 3PB specimen

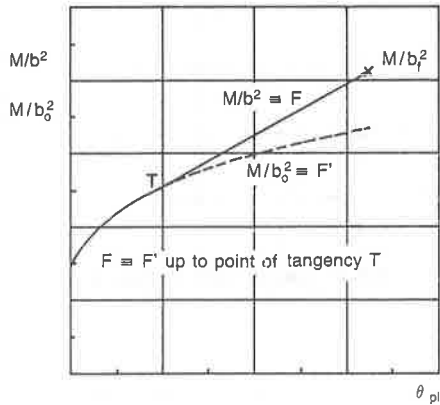


Fig. 2 - Tentative key curve F based on one test result

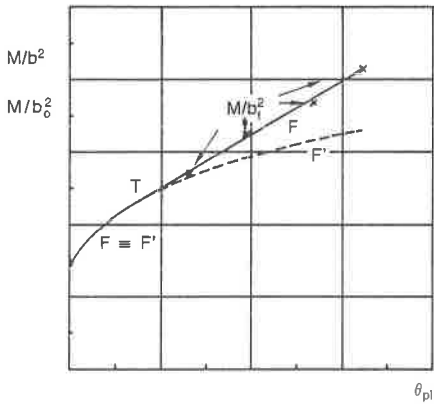


Fig. 3 - Best fitting key curve F using the four test results

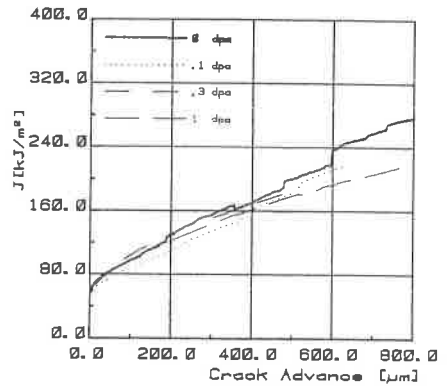


Fig. 4 - Averaged J-resistance curves for the weld metal at 350°C

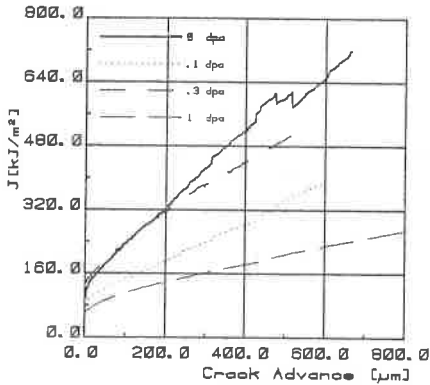


Fig. 5 - Averaged J-resistance curves for the base metal at 550°C

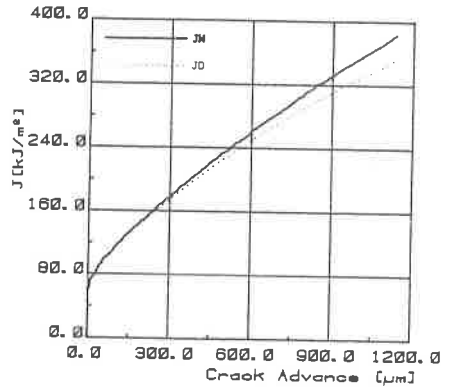


Fig. 6 -  $J_M$  versus  $J_D$ -R curves, weld metal at 350°C, non-irradiated